

Mathematical Model for the transmission of *Plasmodium Vivax* Malaria

Puntani Pongsumpun and I-Ming Tang

Abstract— *Plasmodium vivax* malaria differs from *P. falciparum* malaria in that a person suffering from *P. vivax* malaria can experience relapses of the disease. Between the relapses, the malaria parasite will remain dormant in the liver of the patient, leading to the patient being classified as being in the dormant class. A mathematical model for the transmission of *P. vivax* is developed in which the human population is divided into four classes, the susceptible, the infected, the dormant and the recovered. Two stable equilibrium states, a disease free state E_0 and an endemic state E_1 , are found to be possible. It is found that the E_0 state is stable when a newly defined basic reproduction number R_0 is less than one. If R_0 is more than one then endemic state E_1 is stable. The conditions for the second equilibrium state E_1 to be a stable spiral node are established. It is found that solutions in phase space are trajectories spiraling into the endemic state. The different behaviors of our numerical results are shown for the different values of parameters.

Keywords— basic reproduction number, equilibrium states, local stability, *Plasmodium Vivax* Malaria.

I. INTRODUCTION

THE developmental biology [1] of the parasite *Plasmodium vivax* determines to a great extent the mathematical model needed to describe the transmission cycle of the human disease caused by this parasite. The sporozoites (one of the stages of the malaria parasite) are introduced into the blood stream of the human by the bite of infected mosquitoes. These then move to the liver of the human. Here some of them transform themselves into merozoites, which then invade the blood cells and cause the illness. The remaining sporozoites are transformed into hypnozoites which then lay dormant in the liver. The relapses occur when some of the hypnozoites transform themselves into schizonts and then into merozoites. These new merozoites then reinvade the blood and cause the illness again. These relapses can occur up to three years after the initial infection. Only a small number of *P. vivax* merozoites remain in the blood between the relapse episodes. The hypnozoite stage does not occur in the three other types of malaria, *Plasmodium falciparum*, *Plasmodium malariae* and *Plasmodium ovale*.

The absence of the hypnozoite stage in the malaria caused by the *P. falciparum* parasite makes the transmission models used to describe *P. falciparum* malaria invalid for describing the transmission of the malaria caused the *P. vivax* parasite. The reasons for *P. falciparum* malaria to be studied more than *P. vivax* malaria are (1) 90% of the malaria cases in Africa is due to *P. falciparum* malaria, (2) most of the deaths due to malaria (2-3 million a year) occur in Africa [2] and (3) *P. falciparum* malaria is a life threatening disease, while *P. vivax* malaria is not. It was commonly assumed that information about *vivax* could be extrapolated from the *falciparum* research. This assumption was challenged at a recent conference convened by the Multilateral Initiative on Malaria [3]. The transmission of malaria is usually described by the Ross-MacDonald (RM) model [4]. However, this model is only suitable for the transmission of the *P. falciparum* malaria since it does not contain a role of possible relapses of the illness. One of the present authors (IMT) has introduced a simple mathematical model [5] to describe the transmission of *P. vivax* malaria. In the model, we included a dormant class in which there are no merozoites in the blood, only dormant hypnozoites in the liver. A person can be reinfected when the hypnozoites are activated.

We wish to look at the model again. In the present state of concern for medical safety, there is no place for human experimentation to see what would happen if new therapies were adopted. Mathematical modeling allows one to simulate what would occur. We introduce in Section 2, the modification of the RM model which would make it applicable to the transmission of *P. vivax* malaria. In Section 3, we analyze our model and simulate the consequences of changing the rate of relapse and other parameters in the model. We discuss in Section 4, the implication of the insights obtained from the simulations. Part of the urgency for doing research on *P. vivax* malaria is due to the fact that *P. vivax* malaria is becoming an emerging public health problem. It is estimated that about 50% of the malaria cases outside of Africa and 10% in Africa are due to *P. vivax* and that the percentages are rising.

II. TRANSMISSION MODEL

The mathematical modeling of the epidemiology of malaria (*P. falciparum*) was started by Ross [6] in 1911 and improved on by MacDonald [7]. In the Ross model, an individual in the human population is classified as being in a non-infected or infected state. This gives rise to what is known as a SIS (susceptible-infected-susceptible) model. It has been suggested [7] that the human population should instead be divided into three states; non-infected, infected but without

Manuscript received October 29, 2006; Revised Manuscript received March 5, 2007.

P.Pongsumpun is with the Department of Mathematics and Computer Science, Faculty of Science, King Mongkut's Institute of Technology Ladkrabang, Chalongkrung road, Ladkrabang, Bangkok 10520, Thailand (corresponding author: phone: 66(2) -737-3000 ext.6196; fax 66(2)-326-4341 ext.284; e-mail: kppuntan@kmitl.ac.th).

I.M.Tang is with the Department of Physics, Faculty of Science, Mahidol University, Rama VI Road, Bangkok 10400, Thailand.

any acute clinical signs, infected with acute clinical sign, to better reflect the clinical status of the individual. Others believe that the population should be divided into susceptible, infected but not infectious and infected and infectious.

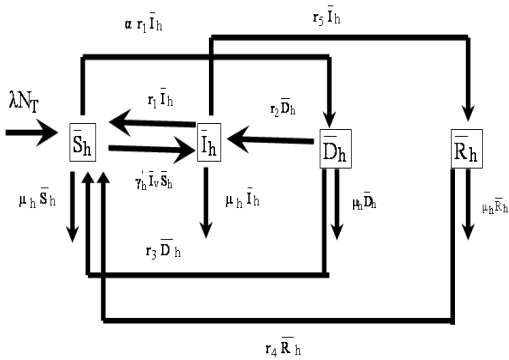


Fig.1. Flow chart of the model.

In our model for the transmission of *P. vivax*, we divide the host (human) population into susceptible (\bar{S}_h), infected (\bar{I}_h), dormant (\bar{D}_h) and recovered (\bar{R}_h) classes. The last category, the recovered are susceptible to further infections and so they reenter into the \bar{S}_h class. In Figure 1, we show the flow chart describing what is occurring in the human population. As we see, λN_T humans are entering into the susceptible class through birth and $(1-\alpha)r_1 \bar{I}_h$, $r_3 \bar{D}_h$ and $r_6 \bar{R}_h(t)$ through the recovery of members of the infected and dormant categories (with λ being the birth rate; N_T , the total human population; r_1 , the recovery rate of a person in the infected category; r_3 , the recovery rate of a member of the dormant population and α being the percentage of infected people in whom some hypnozoites remain dormant in the liver). $(1-\alpha)$ is the percentage of infected humans who recover and become susceptible again. The time rate of change of the number of susceptible members is equal to the number entering minus the number leaving. This gives us the following differential equation for the time rate of change of the susceptible population;

$$\frac{d}{dt} \bar{S}_h(t) = \lambda N_T + r_3 \bar{D}_h(t) + (1-\alpha)r_1 \bar{I}_h(t) - \gamma'_h \bar{I}_v(t) \bar{S}_h(t) - \mu_h \bar{S}_h(t) + r_4 \bar{R}_h(t) \tag{1a}$$

Applying similar considerations to the other population classes, we obtain

$$\frac{d}{dt} \bar{I}_h(t) = \gamma'_h \bar{I}_v(t) \bar{S}_h(t) - (r_1 + \mu_h) \bar{I}_h(t) + r_2 \bar{D}_h(t) - r_5 \bar{I}_h(t), \tag{1b}$$

$$\frac{d}{dt} \bar{D}_h(t) = \alpha r_1 \bar{I}_h(t) - (r_2 + r_3 + \mu_h) \bar{D}_h(t) \tag{1c}$$

and

$$\frac{d}{dt} \bar{R}_h(t) = r_5 \bar{I}_h(t) - (r_4 + \mu_h) \bar{R}_h(t) \tag{1d}$$

where the parameters in the above equations are defined as

- λ is the birth rate of human population,
- μ_h is the death rate of human population,
- N_T is the total number of human population,
- α is the percentage of infected human in whom some hypnozoites remain dormant in the liver,
- r_1 is the rate at which a person leaves the infected class by recovering or by entering into the dormant class,
- r_2 is the rate at which the dormant human relapses back to the infected human,
- r_3 is the recovery rate of the dormant human,
- r_4 is the rate at which the recovered human relapses back to the susceptible human, and
- r_5 is the rate at which the infected human recovers, since *P. vivax* infection is non lethal, the death rates will be the same for all human classes and we will have $N_T = \bar{S}_h + \bar{I}_h + \bar{D}_h + \bar{R}_h$

Equation (1a) also contains the term $\gamma'_h \bar{I}_v(t) \bar{S}_h(t)$. This term represents the lost of the susceptible person due to a bite of a infected mosquitoes. γ'_h is the rate at which the *P. vivax* parasite is transmitted from the mosquito to the human and is given by [8]

$$\gamma'_h = b \frac{\beta_h}{N_T + m} \tag{2}$$

where b is the specie-dependent biting rate of the mosquitoes; m is the population of other animals that the mosquitoes can feed on and β_h is the probability the parasite passed on by the mosquito will continue to thrive in the human. β_h depends partly on the immune response of the host to the infection. \bar{I}_v is the number of infected mosquitoes. The dynamics of the mosquitoes populations are given by

$$\frac{d\bar{S}_v}{dt} = A - \gamma'_v \bar{S}_v(t) \bar{I}_h(t) - \mu_v \bar{S}_v(t) \tag{3a}$$

and

$$\frac{d\bar{I}_v}{dt} = \gamma'_v \bar{S}_v(t) \bar{I}_h(t) - \mu_v \bar{I}_v(t). \tag{3b}$$

At equilibrium, the total number of female mosquitoes will be A/μ_v . A is the rate at which the mosquitoes are recruited and μ_v is the death rate for the mosquitoes. It should be noted that a mosquito can not be infected through a bite of a human belonging to the dormant class. γ'_v is the rate at which the mosquitoes become infected with the Plasmodium Vivax parasite once the mosquito has bitten an infected human. We also assume $N_V = \bar{S}_v + \bar{I}_v$. The working equations of the model are obtained by dividing (1a), (1b), (1c) and (1d) by N_T and (3a) and (3b) by A/μ_v . This would give us six equations expressed in terms of the renormalized variables;

$$S_h = \bar{S}_h/N_T, I_h = \bar{I}_h/N_T, R_h = \bar{R}_h/N_T,$$

$$S_v = \bar{S}_v/(A/\mu_v) \text{ and } I_v = \bar{I}_v/(A/\mu_v).$$

The conditions $S_h + I_h + D_h + R_h = 1$ and $S_v + I_v = 1$, leads to only four of these equations being needed. We pick the four equations to be

$$\begin{aligned} \frac{d}{dt} S_h(t) &= \mu_h + r_3 D_h(t) + (1-\alpha)r_1 I_h(t) \\ &\quad - \gamma_h I_v S_h(t) - \mu_h S_h(t) \\ &\quad + r_4(1 - S_h(t) - I_h(t) - D_h(t)) \end{aligned} \tag{4a}$$

$$\begin{aligned} \frac{d}{dt} I_h(t) &= \gamma_h I_v S_h(t) - (r_1 + \mu_h) I_h(t) + r_2 D_h(t) \\ &\quad - r_5 I_h(t) + r_5(1 - S_h(t) - I_h(t) - D_h(t)) \end{aligned} \tag{4b}$$

$$\frac{d}{dt} D_h(t) = \alpha r_1 I_h(t) - (r_2 + r_3 + \mu_h) D_h(t) \tag{4c}$$

and

$$\frac{d}{dt} I_v(t) = \gamma_v(1 - I_v(t))I_h(t) - \mu_v I_v(t) \tag{4d}$$

where the new transmission rates are $\gamma_h = \gamma'_h(A/\mu_v)$ and $\gamma_v = \gamma'_v N_T$. The domain of solutions is

$$\Omega = \{(S_h, I_h, D_h, S_v, I_v) \mid 0 \leq S_h + I_h + D_h \leq 1, 0 \leq S_v + I_v \leq 1\}$$

III. ANALYSIS OF THE MATHEMATICAL MODEL

A. Analytical Results

To find the equilibrium points, we set the RHX's of (4a) to (4d) to zero. Doing this, we get

- i) the disease free equilibrium state $E_0 = (1, 0, 0, 0)$
- ii) the endemic equilibrium state

$$E_1 = (S_h^*, I_h^*, D_h^*, I_v^*)$$

where

$$S_h^* = \frac{BN}{\gamma_v \mu_{h_{23}} \mu_{h_{46}} P},$$

$$I_h^* = \frac{X_0 - R}{\gamma_v P},$$

$$D_h^* = \frac{(\alpha \mu_{h_{46}} r_1)(X_0 - R)}{\gamma_v \mu_{h_{23}} \mu_{h_{46}} P},$$

$$I_v^* = \frac{X_0 - R}{B \gamma_h} \tag{5}$$

with

$$N = \mu_{h_{46}} (\mu_h (\mu_h + r_{13}) + r_1 (r_2 (1-\alpha) + r_3))$$

$$+ (\mu_h (\mu_h + r_{26}) + r_2 r_4 + r_3 r_6) r_5,$$

$$B = \mu_{h_{46}} (\mu_h (\mu_v + \gamma_v) + \alpha \mu_v r_1 + (\mu_v + r_v)(r_2 + r_3)) + \mu_v (\mu_{h_{23}} + r_4) r_5,$$

$$\begin{aligned} P &= \mu_{h_{46}} (\gamma_h (\mu_{h_{23}} + \alpha r_1) + \mu_h (\mu_h + r_{13}) \\ &\quad + r_1 (r_2 (1-\alpha) + r_3)) + (\mu_h (\mu_h + r_{26}) \\ &\quad + \gamma_h \mu_{h_{23}} + r_2 r_4 + r_3 r_4) r_5, \end{aligned}$$

$$X_0 = \mu_{h_{46}} (\gamma_h \gamma_v \mu_{h_{23}} + \alpha \mu_v r_1 r_2), \tag{4a}$$

$$R = \mu_v (\mu_{h_{46}} (\mu_h (\mu_h + r_{13}) + r_1 (r_2 + r_3)) + (\mu_h (\mu_h + r_{26}) + r_2 r_4 + r_3 r_4) r_5)$$

where $\mu_{h_{23}} = \mu_h + r_2 + r_3,$

$$\mu_{h_{46}} = \mu_h + r_4,$$

$$r_{13} = r_1 + r_2 + r_3$$

$$r_{26} = r_2 + r_3 + r_4. \tag{6}$$

We observe that endemic equilibrium point exists when

$$X_0 > R \text{ or } \frac{X_0}{R} > 1.$$

The local stability of each equilibrium point is determined by the sign of all eigenvalues. If all eigenvalues have negative real parts, then that equilibrium point is locally stable. Eigenvalues for each equilibrium point are obtained by setting

$$\det(J - \lambda I) = 0 \tag{7}$$

where J is the gradient matrix evaluated at the equilibrium point.

The correspondent eigenvalues for each equilibrium point are found by solving the characteristic equation; which is in the form

$$\lambda^4 + s_3 \lambda^3 + s_2 \lambda^2 + s_1 \lambda + s_0 = 0 \tag{8}$$

By using Routh-Hurwitz criteria [9], each equilibrium point is locally stable if the following conditions are satisfied;

$$\text{i) } s_3 > 0, \tag{9}$$

$$\text{ii) } s_1 > 0, \tag{10}$$

$$\text{iii) } s_0 > 0, \tag{11}$$

$$\text{iv) } s_3 s_2 s_1 > s_1^2 + s_3^2 s_0 \tag{12}$$

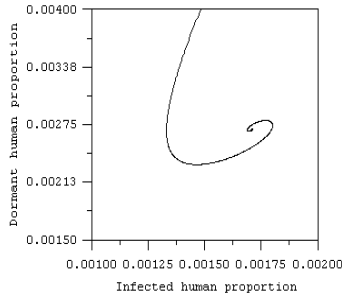
We check the above conditions by using MATHEMATICA (Wolfram Research, Champaign, IL), then we found that E_0 is locally stable for $R_0 < 1$ and E_1 is locally stable for

$$R_0 > 1; \text{ where } R_0 = \frac{X_0}{R}.$$

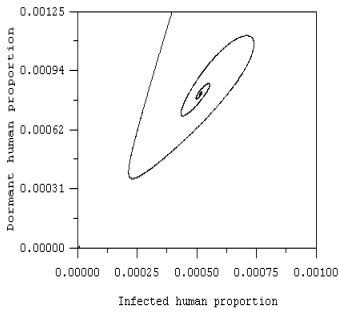
B. Numerical Results

In this section, we compare the susceptible of our model for the different parameters.

Case I, r_4 is changed and the other parameters are fixed.



2(a)



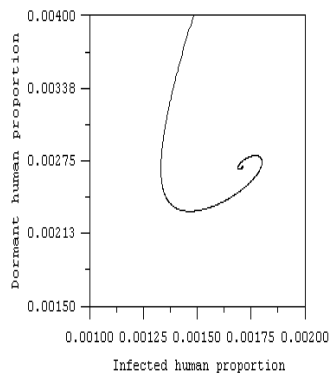
2(b)

Fig.2(a). Behavior of our model for $r_4 = 1/(365 * 5)^{-1}$ day, $R_0 = 38.6$.

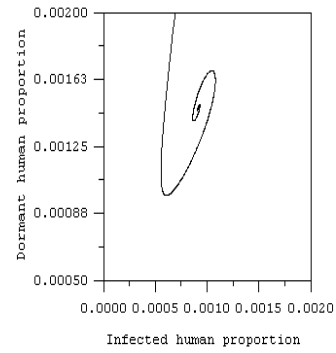
(b). Behavior of our model for $r_4 = 1/(365 * 20)^{-1}$ day, $R_0 = 38.7$.

The other similar parameters for fig.2(a) and fig.2(b) are $r_1 = 1/14^{-1}$ day, $r_2 = 1/(365 * 5)^{-1}$ day, $\mu_h = 1/(365 * 70)^{-1}$ day, $r_3 = 1/30^{-1}$ day, $\alpha = 0.75$, $\mu_v = 0.04$, $\gamma_h = 2.5$, $\gamma_v = 0.25$, $r_5 = 1/3^{-1}$ day, $\mu_h = 1/(365 * 70)$.

Case II, r_2 and r_4 are changed and the other parameters are fixed.



3(a)



3(b)

Fig.3(a) Behavior of our model for $r_2 = 1/(365 * 5)^{-1}$ day,

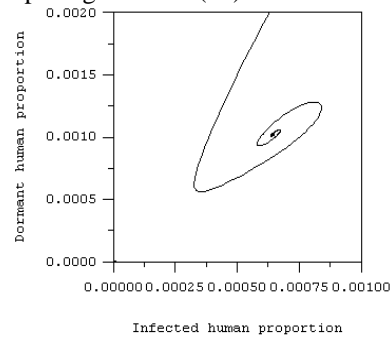
$r_4 = 1/(365 * 5)^{-1}$ day and $R_0 = 38.6$.

(b) Behavior of our model for

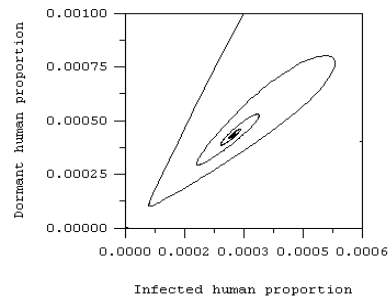
$r_2 = 1/(365 * 20)^{-1}$ day, $r_4 = 1/(365 * 10)^{-1}$ day and $R_0 = 38.5$.

The other similar parameters for fig.3(a) and fig.3(b) are $r_1 = 1/14^{-1}$ day, $\mu_h = 1/(365 * 70)^{-1}$ day, $r_3 = 1/30^{-1}$ day, $\alpha = 0.75$, $\mu_v = 0.04$, $\gamma_h = 2.5$, $\gamma_v = 0.25$, $r_5 = 1/3^{-1}$ day.

Case III, When we input the effect of time delay into our model. In this case, the members of the dormant class do not relapse until a passage of time (τ).



4a)



4b)

Fig.4(a) Behavior of our model for $r_4 = 1/(365 * 15)^{-1}$ day and $\tau = 365 * 30$ day.

(b) Behavior of our model for $r_4 = 1/(365 * 50)^{-1}$ day and $\tau = 365 * 50$ day.

The other similar parameters for fig.4(a) and fig.4(b) are $r_1 = 1/14^{-1}$ day, $\mu_h = 1/(365 * 70)^{-1}$ day, $r_2 = 1/(365 * 5)^{-1}$ day, $r_3 = 1/30^{-1}$ day, $\alpha = 0.75$, $\mu_v = 0.04$, $\gamma_h = 2.5$, $\gamma_v = 0.25$, $r_5 = 1/3^{-1}$ day.

IV. CONCLUSION

In this study, we have compared the results of the simulation when different values of several parameters are used. Figures 2 to 4 show the trajectories of the behaviors in (human) infected-dormant vector space. They all indicate a spiraling of the trajectories into the endemic state. Each pair of figures 2a) & 2b), 3a) & 3b) and 4a) & 4b) shows the behavior when the parameter is changed. When the time at which the recovered human relapses back to the susceptible human is longer, the spiraling in is more severe as shown in figure 2. When the time at which the dormant human relapses back to the infected human is longer than the time at which the recovered human relapses back to the susceptible human, the spiral pattern is more severe.

We have also looked at the effects of there being a time delay before a person in the dormant class relapses into the infected class, i.e., the symptoms returns. We have simulated the course of the disease (malaria) delay time is changed. In Figure 4, we show the results of our numerical simulation. As we see, when the time delay is longer, the spiral pattern is more severe.

ACKNOWLEDGMENT

This work is supported by Commission on Higher Education and the Thailand Research Fund according to contract number MRG5080078.

REFERENCES

- [1] Garnhan PCC., *Malaria parasites of man: life-cycles and morphology (excluding ultrastructure)* IN W.H. Wernsdorfer and I. McGregor (Eds), *Malaria*, Churchill Livingstone, Edinburg, 1988.
- [2] WHO, *World Malaria Situation in 1994: Weekly Epidemiological Record*, Geneva, 1997.
- [3] Sina B., "Focus on Plasmodium Vivax," *Trends in Parasitology*, vol.18, pp.287-289, 2002.
- [4] Anderson RM. and May RM., *Infectious Disease of Humans, Dynamics and Control*. Oxford U. Press, Oxford, 1991.
- [5] Kammanee A., Kanyamee N. and Tang IM., "Basic Reproduction Number for the Transmission of *Plasmodium Vivax* Malaria," *Southeast Asian Journal of Tropical Medicine and Public Health*, vol.32, pp.702-706, 2001.
- [6] Ross R., *The prevention of Malaria*, 2th ed. Murray, London, 1911.
- [7] MacDonald G., *The epidemiology and control of malaria*. Oxford University Press, London, 1957.
- [8] Esteva L., Vargus C., "Analysis of a dengue disease transmission model," *Mathematical Bioscience*, vol.150, pp.131-151, 1998.
- [9] J.E. Marsden, M. McCracken, *The Hopf Bifurcation and its application*. Springer-Verlag: New York, 1976